PHYSICAL REVIEW D VOLUME 22, NUMBER 10 15 NOVEMBER 1980

Topological excitations and Monte Carlo simulation of Abelian gauge theory

T. A. DeGrand
Department of Physics, University of California, Santa Barbara, California 93106

Doug Toussaint
Department of Physics, and Institute for Theoretical Physics, University of California, Santa Barbara, California 93106

(Received 24 June 1980)

We study the phase structure of lattice electrodynamics in three and four dimensions using Monte Carlo simulation, with special emphasis on the topological excitations of the theory. We formulate an operational definition of a monopole and measure the density of monopoles as a function of coupling constant. In three dimensions and for strong coupling in four dimensions monopoles screen external magnetic fields. Below a critical coupling in four dimensions the external field penetrates into the bulk of the medium; this long-range correlation essentially shows that the lattice theory in weak coupling is characterized by a massless photon.

I. INTRODUCTION

Lattice gauge theories provide an attractive way of studying the strong-coupling behavior of gauge theories.[1] Even the simplest such theory, where the internal symmetry group is U(1), is of theoretical interest. In three dimensions this theory shows confinement for all values of the coupling. This behavior can be understood as the result of topological excitations in the theory.[2,3] In four dimensions the theory must have two phases.[4] The high-temperature phase, common to all lattice gauge theories, is a confining phase. The low-temperature phase provides the continuum limit of the theory. If the continuum limit is to be free electrodynamics, then the low-temperature phase must be somewhat special; it must contain a massless photon.

The recent work of Creutz, Jacobs, and Rebbi[5] and of other authors[6] has shown that Monte Carlo simulation is a valuable tool for investigating gauge theories. In this paper we describe a Monte Carlo study of Abelian lattice gauge theory from the point of view of the topological excitations.

In three dimensions the topological excitations are pointlike magnetic monopoles. Using an operational definition of a magnetic monopole, we find that our Monte Carlo simulations do contain monopoles. We then impose boundary conditions corresponding to immersing the system in an external magnetic field and find that the monopoles move in such a way as to screen the field. All this is exactly as expected; the strong-coupling phase is like a magnetic superconductor where electric flux is confined to flux tubes, and magnetic fields are screened.

In four dimensions the topological excitations are strings of monopole current. It is thought that the phase transition in the four-dimensional theory arises from the unbinding of closed loops of monopole string.[3] We find that when an external magnetic field is applied to a four-dimensional system there is a dramatic change in its behavior at $1/e^2 = \beta \approx 0.99-1.00$. For smaller β the field is shielded, while for larger β a finite field penetrates the bulk of the material. Thus, by observing a long-range field, we obtain a direct verification of the transition to a Coulomb phase.

Most of our calculations have used the Wilson form of the action. In this form the partition function is

$$Z_{\text{Wilson}} = \int [d\Theta_\mu(r)] \exp\left[\beta \sum_{r,\mu<\nu} \cos\Theta_{\mu\nu}(r)\right], \quad (1.1)$$

where Θ_μ is the angular variable associated with the link at r in the μ direction and

$$\Theta_{\mu\nu}(r) = \Theta_\mu(r) + \Theta_\nu(r+\hat{\mu}) - \Theta_\mu(r+\hat{\nu}) - \Theta_\nu(r)$$

is the sum of the four angles around the unit plaquette. In this form the theory has a phase transition at $\beta \approx 0.99$. We have also carried out some simulations using the Villain form of the partition function,

$$Z_{\text{Villain}} = \int [d\Theta] \sum_{r,\mu<\nu} \sum_{n=-\infty}^{\infty} \exp[-\tfrac{1}{2}\beta(\Theta_{\mu\nu}(r) - 2n\pi)^2] \quad (1.2)$$

We find that this action yields the same qualitative behavior as the Wilson action [Eq. (1.1)], but the transition point is at $\beta_c \approx 0.62$.

The internal symmetry group under which Θ transforms is chosen to be $Z(N)$ with N large—50–200, typically. $Z(N)$ theories for $N \geq 6$ are known to have three phases—a low-β electrically confining phase, a medium-β phase which is presumed to be Coulombic, and a very-large-β phase

which is magnetically confining.[5,7] The high-β critical point is known to be proportional to N^2 so that for the large N's studied here it occurs at β much too high to be seen. So the $Z(N)$ theories are equivalent to U(1) for all practical purposes, and we shall often refer to them as such.

Our interest in $Z(N)$ rather than U(1) symmetry is purely technical. The time required for performing computations is considerably shortened, allowing us to study larger systems than would otherwise be possible. With this preparation we turn to the actual computations.

In Sec. II we briefly discuss Monte Carlo simulation of U(1) gauge theory. In Sec. III we describe how to find topological excitations in Monte Carlo data, and Sec. IV is an analysis of the behavior of these systems in external magnetic fields. Our conclusions are summarized in Sec. V. Some technical details of our Monte Carlo methods and a review of some simple theoretical ideas about monopoles are relegated to the appendices.

II. MONTE CARLO SIMULATION

The aim of Monte Carlo simulation is to generate a sequence of configurations for the system in such a way that the probability of producing a given configuration is given by Boltzmann weighting. That is, if two configurations have actions S_1 and S_2, the ratio of the probabilities of finding the configurations should be

$$\frac{P_1}{P_2} = \exp(S_1 - S_2) . \tag{2.1}$$

Monte Carlo simulations typically generate new configurations from old configurations by changing one variable at a time according to an algorithm designed to reproduce the configuration weighting (2.1) after many cycles. This process is repeated for every variable in the system. (Application of the algorithm to every variable in the system will be called "a pass through the system.") We use the standard Metropolis method for generating configurations.[8] After a sufficient number of passes for the system to each equilibrium (i.e., to become essentially independent of the starting configuration) expectation values of physical quantities may be measured by averaging their values over many successive configurations. Because configurations on successive passes are highly correlated, it is convenient to make several passes through the system between measurements. Further comments on our Monte Carlo program will be deferred until Appendix A.

Perhaps the most fundamental quantity that can be measured is the average energy (action). This quantity was extensively studied in the original work of Creutz, Jacobs, and Rebbi.[5] In three dimensions the energy is an entirely smooth function of the inverse temperature β, consistent with a one-phase structure. In four dimensions the energy shows pronounced hysteresis for β near 1, as expected if there is a phase transition there. One can test whether the putative phase transition is first order or continuous by beginning with a completely random or completely ordered initial configuration, presumably typical of the large- and small-β phases, and watching the energy as a function of the number of passes through the lattice. As shown in Fig. 1 and in the results of Creutz *et al.*,[5] the internal energy in the two cases converges to a common value, indicating that the phase transition is continuous.

The standard probe of the physics of a lattice gauge theory is the Wilson loop,

$$W(C) = \left\langle \mathrm{Tr} \sum_{i \in C} U_i \right\rangle . \tag{2.2}$$

Expectation values of small Wilson loops can easily be evaluated in a Monte Carlo simulation. We expect that in a confining phase large Wilson loops will be proportional to exp(−area), while in a phase with free charge large loops behave as exp(−perimeter). The expectation values of small loops in four dimensions are graphed in Fig. 2. For small β, these small loops show an area-law behavior. However, for $\beta > 1$ the behavior is unclear. Our data for loops up to 3×3 for $\beta > 1$ do not fit well to any simple form. We expect small loops to show large corrections to the asymptotic form in a phase with massless particles.[9] Clearly, we want better indicators of the nature of the phases than small Wilson loops. To find such indicators we turn to a study of the topological excitations of the theory, monopoles in three dimensions, and monopole strings in four dimensions.

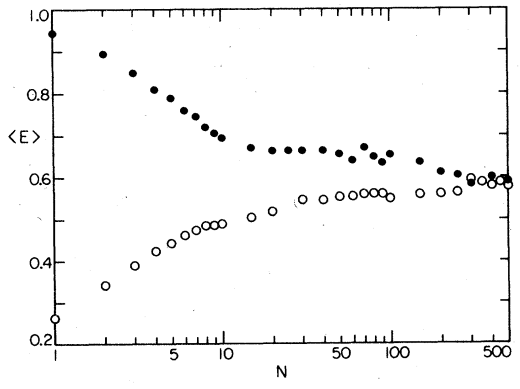

FIG. 1. Internal energy $\langle E \rangle$ vs N, the pass number, for a 6^4 $Z(100)$ system at $\beta = 0.99$, very close to the critical temperature.

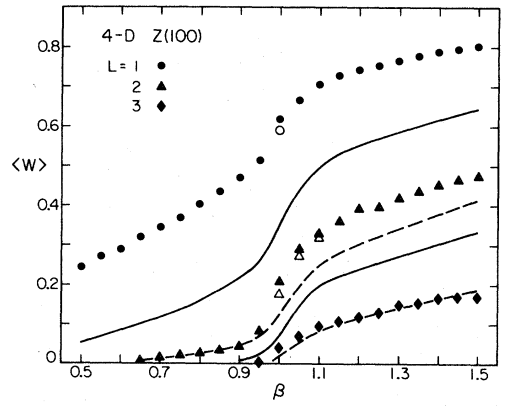

FIG. 2. Wilson loops of size $L \times L$ in $Z(100)$ on a 5^4 lattice, for $L = 1, 2, 3$. The smooth lines are direct extrapolations of a perimeter law from one L to $L+1$; the broken lines are extrapolations of an area law. Closed symbols represent data taken in runs where β decreased; open symbols show data taken in runs where β increased, for β near β_c, where hysteresis is seen.

III. MONOPOLES IN LATTICE THEORIES

It is well known that confinement in three-dimensional Abelian gauge theories can be understood in terms of magnetic monopoles. This is true both in lattice gauge theory with a compact gauge group[3] and in a continuum theory where the U(1) symmetry results from the breaking of a compact group via the Higgs mechanism.[2] This mechanism may be analogous to the effects of instantons or merons in four-dimensional non-Abelian theories.[10] The analysis of three-dimensional lattice theory by Banks, Myerson, and Kogut,[3] which follows the analysis of the two-dimensional XY model by José, Kadanoff, Kirkpatrick, and Nelson,[11] proceeds by performing a series of transformations on the partition function for the Villain form of the theory which explicitly decompose the functional integral into Gaussian integrals and an integral over a monopole field. This monopole field is defined in the boxes (three-cubes) of the theory where it takes integer values, and interacts with itself via the lattice Coulomb potential. Confinement is then understood in terms of the disordering of the theory by free pseudoparticles. In four dimensions the topological excitations are strings (world lines) of monopole current. Consideration of entropy and energy suggests that the phase transition at large coupling can be understood as the unbinding of loops of monopole current to form a condensate.

We are naturally led to ask whether monopoles are present in Monte Carlo simulations and whether the observed behavior of the theory can be understood in terms of these monopoles. We begin with the simplest question: Are there monopoles in three dimensions?

We search for monopoles by using Gauss's law. By measuring the total magnetic flux emanating from a closed surface in the lattice we can determine whether or not the surface encloses a monopole. For small angles Θ, the flux is defined by

$$ds \cdot B = \sum_{\text{surface}} ds_a \epsilon_{abc} \tfrac{1}{2} (\nabla_b \Theta_c - \nabla_c \Theta_b) = \sum_{\text{surface}} \Theta_p , \quad (3.1)$$

where Θ_p is the oriented plaquette angle, a gauge-invariant quantity. Clearly, if we used exactly this definition, we would find a net flux of zero for any closed surface since each link would be included twice, once with each sign. However, our definition of flux should be periodic in the Θ_p. In particular, if the plaquette angle is 2π, the plaquette carries zero energy. Such a configuration should be regarded as a Dirac string passing through the plaquette. Our algorithm for evaluating the flux is as follows. We assume that the plaquette angle $\Theta_{\mu\nu}$ consists of two pieces: physical fluctuations which lie in the range $-\pi$ to π, and Dirac strings which carry 2π units of flux. Defining $\bar{\Theta}_{\mu\nu} = \Theta_{\mu\nu} - 2\pi n_{\mu\nu}$, where $n_{\mu\nu}$ is the number of strings through the plaquette, we measure the monopole number M inside a surface:

$$2\pi M = \sum_{\text{surface}} \bar{\Theta}_{\mu\nu} \quad (3.2)$$

$$= \sum_{\substack{\text{boxes} \\ \text{inside surface}}} \nabla_\mu \epsilon_{\mu\nu\lambda} \bar{\Theta}_{\nu\lambda} \quad (3.3)$$

$$= 2\pi \sum_{\text{boxes}} \epsilon_{\mu\nu\lambda} \nabla_\mu n_{\nu\lambda} . \quad (3.4)$$

Equation (3.3) is the lattice equivalent of $M(x) = \vec{\nabla} \cdot \vec{B}$ and (3.4) says that the monopole number in a volume is given by the net number of Dirac strings entering the volume. It should be clear that adding multiples of 2π to any of the link variables in a configuration can move the Dirac strings around but cannot change the net number entering a volume, and that the monopole number in any volume is the algebraic sum of the monopole numbers of its subvolumes. Therefore, to count the monopoles in our system we examine cubes of unit volume. Examples taken directly from computer data of a monopole configuration and a monopole-antimonopole pair are shown in Fig. 3. By looking at successive Monte Carlo configurations, one can observe the movement of monopoles and the creation and annihilation of monopole-antimonopole pairs.

Because monopoles are collective excitations of many link variables, they move slowly in Monte

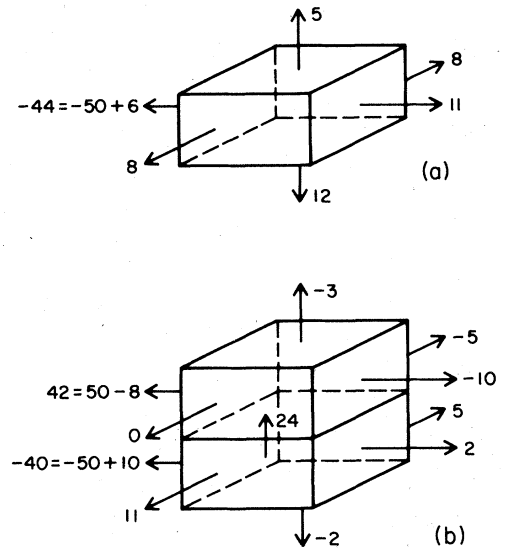

FIG. 3. A monopole (a) and a monopole-antimonopole pair (b) in $Z(50)$. Arrows label the flux out of each face. The strings, carrying ± 50 units of flux, flow through the left-hand faces.

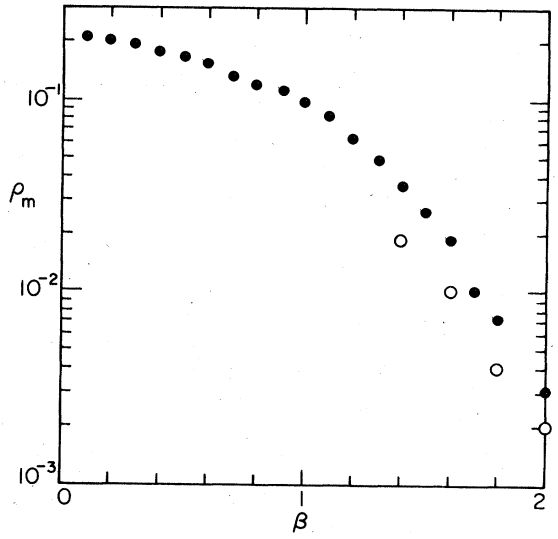

FIG. 4. Monopole density in three dimensions. The solid circles are the total density of monopoles, while the open circles are the density of "isolated" monopoles, for which no adjacent box contains an antimonopole.

Carlo simulations. To change the monopole number inside a surface, or to move the monopole around, at least one plaquette must pass through its maximum energy.

The definition of monopoles used here is similar to a definition of vortices in the XY model used in Monte Carlo calculations by Chester and Tobochnik.[12] It should be emphasized that our decomposition of a particular configuration into monopoles and fluctuations is not exactly the same as Banks, Myerson, and Kogut's decomposition of the functional integral into integrations over Gaussian variables and monopole variables. It is only at very large β (low temperature), where monopoles are heavy and Gaussian fluctuations really are small, that the two decompositions should coincide. Among other differences, the monopole field defined by Banks, Myerson, and Kogut can take on all integral values, while the monopole number used here is kinematically limited to be no larger than two in a unit cube.

The simplest measurement we can make is the density of monopoles. The average density of monopoles or antimonopoles $\rho_m = \frac{1}{2}(\langle N_M{}^+\rangle + \langle N_M{}^-\rangle)/V$ as a function of β is displayed in Fig. 4. It is seen to be a smoothly falling function of β. For the range of β in which Monte Carlo calculations are practical, most of the monopoles and antimonopoles are in pairs, with a monopole and antimonopole in adjacent boxes. Figure 4 also shows the density of "isolated" monopoles—those for which none of the neighboring cubes contains an antimonopole. It can be seen that as β increases, the density of close pairs falls off more rapidly than the density of isolated monopoles. Both the density of pairs and the density of isolated monopoles appear to be falling off exponentially with slopes in reasonable agreement with theoretical estimates using the Villain form or the dilute-gas approximation (DGA). These estimates are discussed in Appendices B and C. Finally we remark that for $\beta > 1$, nearly all our monopoles have $M = \pm 1$. At lower β, occasional $M = \pm 2$ monopoles are seen. Simple arguments suggest $\rho_{M=2} \approx \rho_{M=1}{}^4$, so it is not surprising that double monopoles are scarce objects.

The pointlike typological excitations in three dimensions become one-dimensional objects in four dimensions. These objects are the world lines of three-dimensional monopoles, or continuous strings of monopole current. The presence of a monopole current in a given direction at any point in space may be found by the same method used in three dimensions, simply measuring the flux (or counting Dirac strings) flowing through a three-dimensional surface oriented normally to the current. That is, we measure

$$2\pi M_\mu(x) = \epsilon_{\mu\nu\alpha\beta}\nabla_\nu \bar{\Theta}_{\alpha\beta}(x) \tag{3.5}$$

as a test for a monopole current at x. Conservation of topological charge demands that $\partial_\mu M_\mu(x) = 0$, so monopole strings form continuous loops. The study of monopole strings is somewhat more complicated than the study of monopoles. We have not found it profitable to measure the average peri-

meter of a string; rather, we have opted to measure the total perimeter of all the strings in a system. We plot this quantity as a function of β in Fig. 5. At low β, ρ_M is large and slowly varying. Near β_c, ρ_M falls dramatically. For large β, ρ_M falls exponentially and more steeply than in three dimensions. The Villain model predicts $\rho_s \sim e^{-\pi^2\beta}$, which is not inconsistent with our data. This curve encourages us to believe that monopole strings are involved in the phase transition.

IV. MONOPOLES AND EXTERNAL FIELDS

Although entertaining, the mere counting of monopoles does not elucidate their role in determining the properties of the theory. The presence of free monopoles is expected to cause confinement.[2,3] A medium containing free monopoles can be thought of as a magnetic superconductor, where magnetic fields are shielded and electric fields are confined to flux tubes.

The quantity of interest is the polarizability of the monopole gas[13]

$$\chi_{ij} \approx \frac{\partial^2}{\partial B_i \partial B_j} \ln Z , \tag{4.1}$$

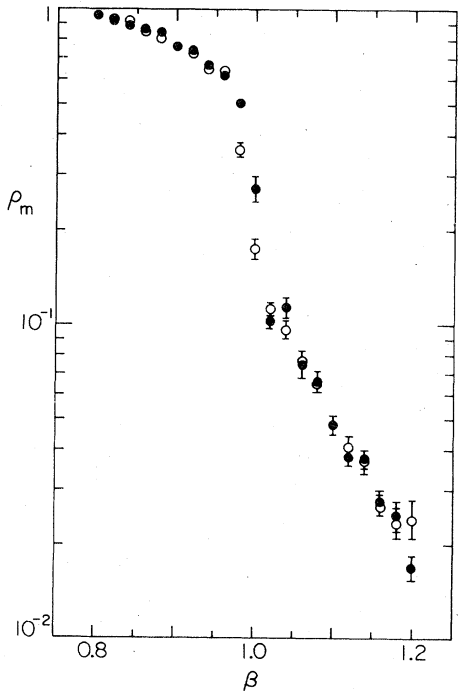

FIG. 5. Expectation value of the monopole string density vs β in $Z(100)$ for a 5^4 lattice. Open circles are found by stepping down in β, closed circles by stepping up in β. At each point the first 50 passes are discarded, then 40 measurements, each separated by five passes, are carried out.

which is proportional to

$$\chi \approx -\sum_r \langle r^2 M(0) M(r) \rangle . \tag{4.2}$$

If the susceptibility is infinite, magnetic fields are shielded. This is what we expect in three dimensions, where the monopoles are unbound for all β. On the other hand, a finite susceptibility corresponds to a renormalization of magnetic charge

$$g_R = g_0/(1+\chi) ,$$

which corresponds to a renormalization of electric charge

$$e_R = (1+\chi) e_0 . \tag{4.3}$$

In principle, the susceptibility could be evaluated in Monte Carlo simulation by directly measuring $\langle r^2 M(0) M(r) \rangle$. However, this quantity involves near cancellations between monopole-monopole contributions and monopole-antimonopole contributions. As a result, it is difficult to evaluate accurately and we experienced little success in our attempts to do so.

A better way to proceed is to introduce an external magnetic field and study the response of the monopoles to it by measuring the field deep inside the system. The magnetic field inside the system will be a sum of the external field and a field generated by the monopoles in terms of a permeability μ, where $\mu = 1+\chi$, $\vec{H}_{\text{external}} = \mu \vec{H}_{\text{internal}}$. For parallel-plate geometry we measure the magnetic flux Φ through planes perpendicular to the external field. Then H is proportional to Φ and a susceptibility may be measured directly:

$$\chi = \frac{\Phi_{\text{external}}}{\Phi_{\text{internal}}} - 1 .$$

We begin by considering three dimensions. Consider a finite cube of a lattice gauge theory, illustrated in Fig. 6, and fix all the plaquette angles on the xy faces to some small value. This amounts to introducing a uniformly distributed magnetic flux through the face. We then put in periodic boundary conditions on the other faces of the cube. However, unless the flux is a multiple of 2π, we must introduce a twist in the boundary conditions.[13-15] That is, when leaving the top (xz) boundary of the cube and reentering the bottom, we add some amount to the links in the x direction. Clearly, the sum of the twist angles on the boundary of a face must equal the magnetic flux through the face modulo 2π. In essence, by fixing the flux at the boundary we have put our medium in a magnetic capacitor. We can now use the Monte Carlo algorithm on this system and measure the location of the monopoles. Equivalently, we may measure the total flux (as defined in Sec. III) through each xy plane.

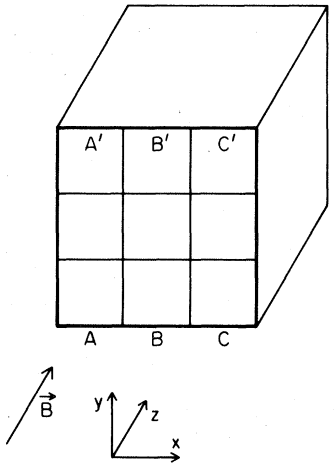

FIG. 6. A finite three-dimensional system. An evenly distributed magnetic flux in the Z direction is imposed by fixing all the plaquette angles on the front face to some value. A "twist" in the boundary conditions involves setting link A' equal to link A plus some increment. Periodic boundary conditions are used in the other two directions.

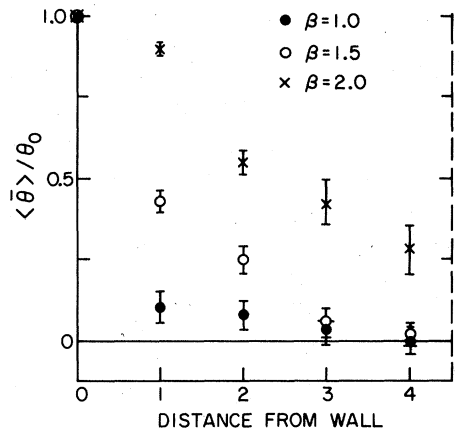

FIG. 7. Screening of a magnetic field in three dimensions in a 10^3 system. The plaquettes in one plane (at the left) are fixed to θ_0, and we plot the expectation value of the reduced angle $\bar{\theta}$ as a function of distance from the fixed plane.

Some of the results of this three-dimensional experiment are shown in Fig. 7. We see that for β of order 1 the magnetic field is screened over a range of one or two lattice spacings. Thus we can actually observe the screening of magnetic charge by the free monopoles in the medium.

In four dimensions the experiment is more interesting. It is easiest to imagine the experimental situation by thinking of three dimensions plus time. For each value of time, we fix plaquettes exactly as in three dimensions. This amounts to embedding the system in an external field oriented in the z direction which is time independent and constant in x and y. We measure the time-averaged flux through planes of constant z. The quantity $\Phi(z)/\Phi(z=0)$ is plotted for two values of β in Fig. 8, using data taken on a $5\times5\times9\times5$ system. At small β the external field is again shielded after a small penetration. However, for $\beta>1$ the situation is completely different. The field in the center of the system is a constant fraction of its value at the edge. Thus the susceptibility is finite, and magnetic charge is renormalized by the monopole strings.

By testing the ability of the medium to support a long-range magnetic field, we are essentially testing for a massless photon. Thus our measurements give a direct verification of the Coulomb phase of U(1) lattice theory.

We have also measured the expectation value of $\sin\Theta_p$ in planes perpendicular to the flux. This is another possible definition of the physical flux and behaves qualitatively like our usual definition.

Clearly the quantity in which we are most interested is the expectation value of the flux at an infinite distance from the plane of fixed plaquettes. Imagine extending our system a long way in the z direction and chopping a segment out of the middle. Information about the bare flux through the system is carried by the twist in the boundary conditions, so we may still carry out the experiment. However, the twist only defines the flux modulo 2π, so we are restricted to fluxes between $-\pi$ and π. We have now arrived at precisely the twisted boundary conditions introduced by 't Hooft[14] and used

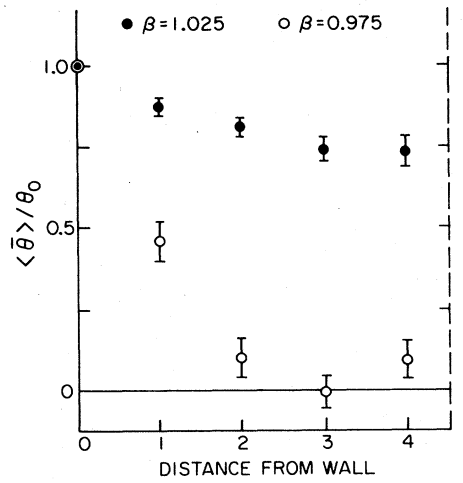

FIG. 8. Screening or penetration of a magnetic field in four dimensions, for two values of β near the phase transition.

in Monte Carlo simulation by Groeneveld *et al.*[15] The advantage of our experiment over that of Ref. 15 is that we are measuring quantities which are linear in the bare flux, while the authors of Ref. 15 studied the energy, which varies quadratically with the bare flux. In Fig. 9 we plot the ratio of renormalized flux to bare flux imposed by twisted boundary conditions as a function of β. The change in character at $\beta \approx 1$ is striking. We estimate from this curve that the transition temperature β_c lies between 0.98 and 1.00. We also plot in Fig. 10 the ratio of $\langle \sin\Theta_{xy} \rangle$ to the bare angle $\sin\Theta_0 = \sin(\text{flux}/N_x N_y)$. Its behavior is qualitatively similar to that of the flux ratio, again showing a long-range field for $\beta > 1$.

Theoretical arguments suggest that the phase transition may occur when the renormalized coupling reaches a universal critical value.[13] This would mean that as β is lowered toward β_c the susceptibility increases to a finite value and then suddenly becomes infinite. In this case we would expect the "renormalized field" that we are measuring to have a discontinuity at β_c. Our data are insufficient to decide whether the flux measured here has such a discontinuity. We repeat that the operational definitions of renormalized flux used here are not quantitatively the same as the definition used in the theoretical arguments, but we can expect them to have qualitatively similar behavior.

We have also carried out some experiments on the Villain form of the theory, where the exponential of the plaquette action is given by

$$\exp[S(\Theta_p)] = \sum_{n=-\infty}^{+\infty} \exp[-\tfrac{1}{2}\beta(\Theta - 2\pi n)^2] . \qquad (4.4)$$

This form of the action is of interest because it lends itself to theoretical analysis. It is in this form of the theory that the partition function can be explicitly decomposed into Gaussian fluctuations and monopole excitations,[3] and it is the Villain form of the action that provides a strikingly good approximation to a fixed line under the Migdal approximate renormalization-group transformation.[11,16] In Fig. 11 we plot $\mu^{-1} = \Phi_{\text{renormalized}}/\Phi_{\text{bare}}$ for this theory, showing a phase transition at $\beta_c \sim 0.62$ or 0.63 and the same sharp behavior of μ as we saw before.

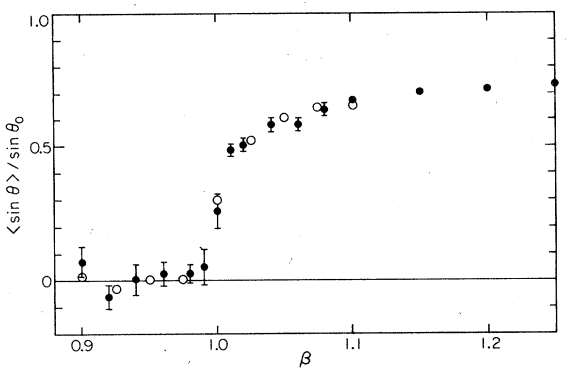

FIG. 10. The expectation value of $\sin\theta_{xy}$ for the same sample. This is another possible definition of the magnetic field.

V. CONCLUSION

In this study of lattice U(1) gauge theory we have demonstrated that it is possible to formulate a description of a monopole which is accessible to measurement in Monte Carlo simulation. We have

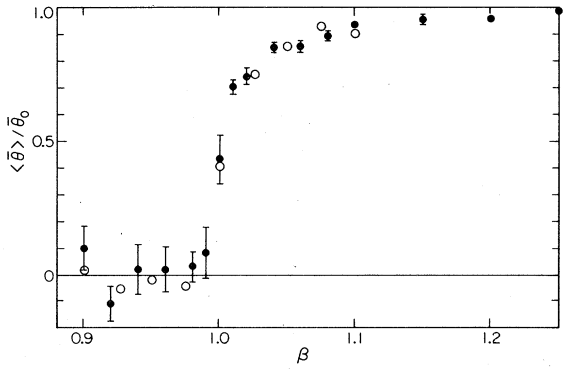

FIG. 9. Expectation value of the reduced plaquette angle $\bar{\theta}_{xy}$ in four dimensions with twisted boundary conditions (solid circles). θ_0 is the angle that the plaquettes would have if the twist angle were evenly distributed over all the plaquettes. The open circles are $\langle \theta \rangle$ in the four central planes of $5\times5\times9\times5$ system with fixed plaquettes on the xy planes of the boundary.

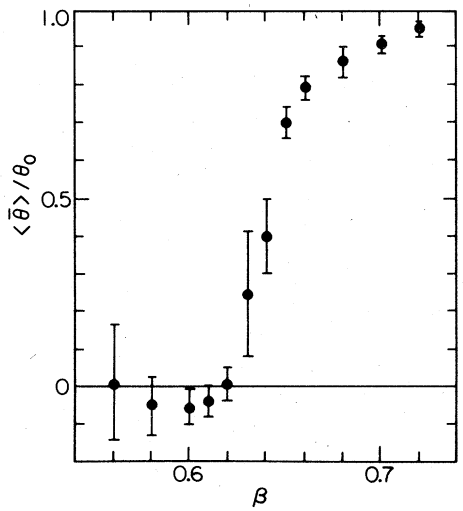

FIG. 11. $\langle \bar{\theta}_{xy} \rangle$ in the Villain form of the theory with twisted boundary conditions.

shown that these monopoles screen external magnetic fields when the theory is in an electrically confining phase. The long-distance penetration of the external field in the high-temperature phase of the four-dimensional theory is evidence that this phase possesses a massless photon. In addition, we are able to measure the renormalization of the external field in the Coulomb phase due to the monopole currents.

Although we have studied systems of only modest size, the nature of the effects we have measured are such that they should be equally valid in systems of infinite extent. In that respect, monopoles and external fields are much better signals for the nature of the phases of a system than are measurements of small Wilson loops whose area and perimeter are of comparable magnitude.

Two extensions of our work suggest themselves. It should be a simple matter to study the Abelian Higgs model in an external field and map the phase boundary between the Higgs/confinement sector and the massless photon sector. It may also be possible to extend the techniques of this paper to studies of topological excitations in non-Abelian gauge or spin theories, monopoles, or instantons. Work on these problems is in progress.

We believe that the results of our studies provide an extremely physical picture of the interplay of topological excitations and critical behavior in lattice photondynamics. Our results also indicate the profitability of using Monte Carlo techniques to study collective excitations of the degrees of freedom of gauge and spin systems.

ACKNOWLEDGMENTS

We thank John Cardy, Sudip Chakravarty, Mike Creutz, Lawrence Jacobs, John Kogut, and Bob Pearson for discussions. This work was supported by the National Science Foundation under Grants Nos. PHY78-08439 and PHY77-27084.

APPENDIX A

This appendix contains some technical comments on our Monte Carlo procedure and on our error estimation procedure. The basic principles of Monte Carlo simulation have been much discussed in the recent literature,[5,6,17] so we concentrate here on some points special to our approach. As noted in the Introduction, we approximated U(1) by $Z(N)$ for N reasonably large. This allowed us to use integer arithmetic in evaluating the plaquette angles. Also, because in $Z(N)$ a plaquette angle has roughly $4N$ possible values, one can simply tabulate all the possible Boltzmann weights at the beginning of the program. Hence no trigonometric functions or exponentials need to be evaluated in the inner loops of the program. We used values of N ranging from 50 to 200 and found no detectable dependence on N.

We used boundary conditions which differ slightly from the usual periodic boundary conditions. Figure 12 illustrates our "skewed" boundary conditions in two dimensions. The blocks represent a finite two-dimensional system replicated an infinite number of times. Ordinary periodic boundary conditions amount to connecting the blocks (really all the same block) as illustrated in Fig. 12(a), while skewed boundary conditions involve connecting the blocks as in Fig. 12(b). Operationally the skewed boundary conditions require that every time one passes out of the right-hand side of the lattice, he reenters the lattice from the left-hand side, but one row higher. In general, when we leave our finite system in the direction of the ith coordinate, we imagine reentering the system with the ith coordinate reset to zero, but the $(i+1)$th coordinate increased by one. The advantage of this method is that all the variables may be arranged in a one-dimensional array $x(j)$. The structure of a d-dimensional lattice is then described by d numbers $J(i)$, $i=1$ to d, which tell how to move one lattice spacing in any direction. The variable which is one unit away from a given variable $x(k_0)$ in the ith direction is simply $x(k_0+J(i))$. The only remaining problem is that this rule may sometimes lead to an index slightly outside the array. This is easily handled by appending a "virtual" copy of the first part of the array onto the end of the array, and appending a copy of the end of the array to the beginning of the array (see Fig. 13). If the action is

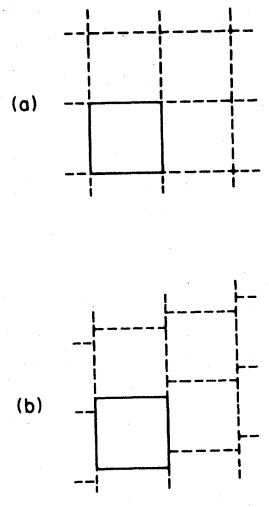

FIG. 12. Periodic boundary conditions. Each square represents a copy of a finite system. (a) Ordinary periodic boundary conditions; (b) skewed boundary conditions.

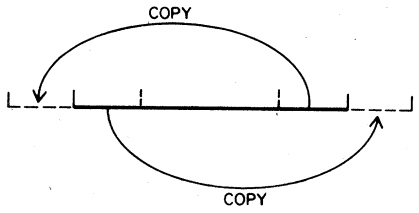

FIG. 13. The virtual lattice. The heavy line indicates the real lattice, stored as a one-dimensional array. The dashed lines indicate the virtual lattice, which is a copy of part of the real lattice.

defined on an elementary plaquette, the fraction of the array that must be duplicated is $1/N$, where N is the size in the most slowly varying direction. Of course, we do not apply the Monte Carlo algorithm to the spins in the virtual array, but simply update them to duplicate the "real" array as necessary.

The advantage of these boundary conditions is that to find a link one site away in the ith direction from the current link we simply add an offset to the index. In contrast, in the most naive implementation of periodic boundary conditions it is necessary to increment one coordinate, reduce it to the correct range (e.g., by the modulo function), and then evaluate a $(d-1)$-order polynomial to locate it anyway, since computer memory is a one-dimensional array. Clearly, the speed advantages of skewed boundary conditions increase rapidly as the number of dimensions increases.

An analogy may help the reader who is confused. Imagine a $10\times10\times10$ spin system where a site is labeled by three integer coordinates between 0 and 9. Placing the digits which label the site side by side (that is, evaluating a polynomial), we find each site labeled by a number between 000 and 999. To translate by n_y units in the y direction, we simply add $0n_y0$ to the number. (Ordinary periodic boundary conditions amount to adding $0n_y0$ with the proviso that all carries are discarded.) In the actual computation, one never needs the three coordinates of a point; everything can be done using the one (three digit) number.

Even in the case of spin systems, skewed boundary conditions are an equally acceptable approximation to an infinite system as standard periodic boundary conditions. For an Abelian gauge theory these two boundary conditions are gauge equivalent. The reason for this is that any configuration that is skewed periodic can be gauge transformed into a configuration which is periodic in the ordinary sense.[13] The only gauge-invariant quantity which can characterize boundary conditions is the Wilson loop going around the entire system.[13]

Clearly, for skewed periodic or ordinary periodic boundary conditions, this Wilson loop is equal to the identity element. However, this loop may be given a nontrivial value by introducing a "twist" in the boundary conditions.[14,15] This can be accomplished, for example, by setting the links along the top edge of the square in Fig. 12 equal to the links on the bottom edge plus some increment. The sum of all these increments, the twist, is gauge invariant and is equal modulo 2π to our usual definition of the magnetic flux through the loop in any particular configuration. With our representation of the lattice, such a twist is easily imposed by adding the increments to the appropriate elements on the virtual lattice illustrated in Fig. 13.

The alert reader may have noted that with skewed boundary conditions a plane that naively divides the lattice—e.g., the plane enclosed by the Wilson loop made up of N steps in the x direction, N steps in the y direction, N steps in the $-x$ direction, and N steps in the $-y$ direction—may not be quite closed. We avoid this problem by choosing the plane defined by the two most slowly varying coordinates when imposing nonzero twists or measuring fluxes. In that plane these annoyances do not occur.

We use the standard Metropolis method for generating configurations.[8,17] When examining a particular variable, we choose a trial value for that variable which lies within a fixed range of the old value. The size of this range is adjusted to provide the desired acceptance ratio (fraction of variables changed in one pass). We used acceptance ratios of 0.4 or 0.5 for most of our work. The efficiency of the simulation appeared largely insensitive to the exact value of the acceptance ratio.

Our programs were written in FORTRAN and run on a VAX 11-780 computer. On this machine one pass through a 5^4 lattice (2500 variables) required 1.5 sec.

Because lattice configurations separated by one Monte Carlo pass are highly correlated, it is advantageous to make several passes between measurements of the quantities to be evaluated. We typically made three to five passes between measurements. Even so, very close to β_c in four dimensions we sometimes observed correlation coefficients of successive measurements as high as 0.8. A typical run used 100 to 200 passes to thermalize the lattice, followed by 200 to 500 passes during which measurements were made.

The statistical uncertainty of a Monte Carlo measurement may be estimated in several ways. The simplest method, valid when correlations are small, is to take the standard deviation of the mean corrected for correlations

$$\Delta x^2 = \frac{1}{N-1}\left(\frac{1}{N}\sum x_i^2 - \bar{x}^2\right)(1+2c_1+\cdots), \quad \text{(A1)}$$

where the x_i are the individual measurements and c_1 is the correlation coefficient of successive measurements

$$c_1 = \frac{\langle x_i x_{i+1}\rangle - \bar{x}^2}{\langle x^2\rangle - \bar{x}^2}. \quad \text{(A2)}$$

The error bars in Fig. 5 were computed in this way. A method which avoids the effect of short-time correlations is to group the sequence of measurements into subsequences, average the subsequences, and compute the standard deviation of the partial averages. When the correlation between successive measurements was small, the two formulas agreed well.

For β very close to β_c in the four-dimensional theory, equilibration takes a very long time. This is especially true for quantities involving collective excitations. Therefore, for the measurements of flux in Figs. 7–11, we made a number of runs (typically 4 to 12) from different starting configurations. The error bars on these figures are obtained from the standard deviations of the averages of the separate runs.

APPENDIX B: MONOPOLES IN THE VILLAIN APPROXIMATION

This appendix recapitulates the transformation of U(1) lattice theory in Villain approximation. It contains no new physics but does serve as a repository for various Villain formulas. The formulas are taken from Banks, Meyerson, and Kogut.[3]

Let us compute the partition function $Z(J)$ in the presence of an external current loop $J_\mu(r)$ for a three-dimensional U(1) theory:

$$Z(J) = \int [d\Theta_\mu(r)] \exp\left[\beta \sum_{r,\mu<\nu} \cos\Theta_{\mu\nu}(r) + i\sum_{r,\mu}\Theta_\mu(r)J_\mu(r)\right], \quad \text{(B1)}$$

where $\Theta_\mu(r)$ is the angle on the μ-directed link at r and

$$\Theta_{\mu\nu}(r) = \partial_\mu\Theta_\nu(r) - \partial_\nu\Theta_\mu(r) \quad \text{(B2)}$$

(all derivatives being finite-difference operators). The Villain approximation consists of making a character expansion on the action

$$e^{\beta\cos\Theta_{\mu\nu}(r)} = \sum_{l_{\mu\nu}=-\infty}^{\infty} e^{il_{\mu\nu}\Theta_{\mu\nu}} I_{l_{\mu\nu}}(\beta), \quad \text{(B3)}$$

combined with the large-β expansion of the modified Bessel function

$$I_l(\beta) \sim e^{-l^2/2\beta}/(2\pi\beta)^{1/2}. \quad \text{(B4)}$$

Inserting (B3) and (B4) into (B1), we evaluate all the Θ_μ integrals and obtain

$$Z(J) \simeq \sum_{r,\mu,\nu,l_{\mu\nu}} \delta_{\partial_\nu l_{\mu\nu} + J_\mu(r),0} \exp\left[-\frac{1}{2\beta}\sum_{r,\mu<\nu} l_{\mu\nu}^2(r)\right]. \quad \text{(B5)}$$

The constraint equation is solved by taking

$$l_{\mu\nu}(r) = n^\mu(n\cdot\partial)^{-1}J^\nu - n^\nu(n\cdot\partial)^{-1}J^\mu + \epsilon_{\mu\nu\lambda}\partial_\lambda l(r), \quad \text{(B6)}$$

where n is a unit vector. Equation (B5) is poorly convergent so we perform a Poisson resummation

$$\sum_{l=-\infty}^{\infty} g(l) = \sum_{m=-\infty}^{\infty}\int d\phi g(\phi)e^{ilm\phi}, \quad \text{(B7)}$$

perform the Gaussian integration over ϕ, and find

$$Z(J) = Z_{\text{monopole}} Z_{\text{spin-wave}} Z_{\text{ext}}, \quad \text{(B8)}$$

where

$$Z_{\text{spin-wave}} = \int [d\phi] \exp\left(-\frac{1}{2\beta}\sum_{r,\lambda}[\partial_\lambda\phi(r)]^2\right), \quad \text{(B9a)}$$

$$Z_{\text{monopole}} = \sum_r \sum_{m(r)=-\infty}^{\infty} \exp\left(-2\pi^2\beta\sum_{r\,\partial\,r'} m(r)V(r-r')m(r') + 2\pi i\sum_{r,r'}\partial_\nu B^\nu(r)V(r-r')m(r')\right), \quad \text{(B9b)}$$

$$Z_{\text{ext}} = \exp\left(-\frac{1}{2\beta}\sum_{r,r',\mu} J_\mu(r)V(r-r')J_\mu(r')\right), \quad \text{(B9c)}$$

and $\nabla^2 V(r-r') = \delta_{r,r'}$; i.e., V is the lattice Coulomb Green's function. $B_\nu(r)$ is the magnetic field generated by J_μ,

$$B_\nu(r) = \epsilon_{\nu\mu\lambda}n_\mu(n\cdot\partial)^{-1}J_\lambda(r) \quad \text{or} \quad \epsilon_{\alpha\beta\gamma}\partial^\beta B^\gamma(r) = J_\alpha(r). \quad \text{(B10)}$$

A Villain monopole is an integer-valued scalar field whose values range from $-\infty$ to ∞ and whose self-interactions and interactions with the external magnetic field are Coulombic.

At large β the density of monopoles is low: Monopoles are widely separated and the density of

monopoles depends in lowest approximation only on their self-interactions. Then the density of isolated monopoles is

$$\rho_M \sim \exp[-2\pi^2\beta V(0)\beta] \tag{B11}$$

and the density of isolated monopole-antimonopole pairs in adjacent lattice sites is

$$\rho_{M\bar{M}} \sim \exp\{-2\pi^2[2V(0) - 2V(1)]\beta\}. \tag{B12}$$

These densities are numerically $\rho_M \sim \exp(-5\beta)$ and $\rho_{M\bar{M}} \sim \exp(-6.58\beta)$, using $V(0) \sim 0.253$ and $V(0) - V(1) = \frac{1}{6}$.

The derivation of a monopole partition function for the four-dimensional theory is essentially identical. Equation (B8) is recovered, with

$$Z_{\text{spin wave}} = \int [dA_\mu] \exp\left(-\frac{1}{2\beta} F_{\mu\nu} F^{\mu\nu}\right) \tag{B13}$$

and

$$Z_{\text{monopole}} = \sum_{r,\mu} \sum_{m_\mu(r)} \delta_{\partial_\mu m_\mu(r),0} \exp\left(-2\pi^2\beta \sum_{\mu,r,r'} m_\mu(r) m^\mu(r') V(r-r') + 2\pi i \sum_{\mu,r,r'} m_\mu(r) V(r-r') \epsilon_{\mu\nu\alpha\beta} n_\nu \partial_\alpha (n\cdot\bar{\partial})^{-1} J_\rho(r')\right) \tag{B14}$$

describing the interaction of closed current loops m_μ with each other and with external fields. At large β the only energetically allowed topological excitations are closed loops of length four. Then

$$\rho_{\text{string}} \sim \exp\{-2\pi^2\beta[4\nu(0) - 4\nu(1)]\}, \tag{B15}$$

but $\nu(0) - \nu(1) = \frac{1}{8}$ so $\rho \sim \exp(-\pi^2\beta)$.

APPENDIX C: SIMPLE DILUTE-GAS APPROXIMATIONS

We can make some simple dilute-gas approximations for monopole densities in three dimensions for β large. The partition function for a system of N boxes

$$Z = \int [d\theta_\mu] \exp\left(\sum_{\text{plaq}} \beta \cos\theta_p\right) \tag{C1}$$

is a function of about $2N$ link variables after gauge fixing. It may be (formally) integrated to give

$$Z(\beta) = \left(\frac{1}{\sqrt{\beta}}\right)^{2N} e^{2N\beta} e^{-S_{\min}} (\det M)^{-1/2}, \tag{C2}$$

where $-S_{\min}$ is the exponent of Eq. (C1) evaluated at some minimum-action configuration and

$$M_{ij} = -\frac{\partial}{\partial\theta_i} \frac{\partial}{\partial\theta_j} \sum_p \cos\theta_p \Big|_{\theta_p = \min} \tag{C3}$$

is the matrix of second derivatives evaluated at the minimum. At large β an absolute minimum is just all $\theta_p = 0$. We may, however, imagine (local) minima of the action which are topologically stable monopole configurations. The density of monopoles in the system will then just be given by the ratio of partition functions evaluated about monopole and vacuum configurations

$$\rho_{\text{monopole}}(\beta) = \frac{Z(\text{monopole})}{Z(\text{vacuum})} = \left(\frac{\det M(\text{mono})}{\det M(\text{vac})}\right)^{-1/2} e^{S(\text{vac}) - S(\text{mono})}. \tag{C4}$$

The action S is proportional to β while the determinants are independent of β. Therefore, at large β the monopole density has the form

$$\rho_M = \exp\left[-\left(m\beta - \tfrac{1}{2} \ln\det \frac{M(\text{mono})}{M(\text{vac})}\right)\right], \tag{C5}$$

where $m\beta$ is a bare monopole mass and the determinants provide the first quantum correction. The determinants are independent of β because at large β the monopole is essentially restricted to lie in the center of a box—i.e., the plaquette angles of the box must all be nearly equal. Therefore, even the putative translation modes become Gaussian.

This approximation to the monopole density becomes valid when the motion of a monopole from one box to another requires tunneling through a high barrier. In this limit Monte Carlo calculations become impractical because the fluctuations in the positions of monopoles from pass to pass become tiny and the system thermalizes slowly. Therefore, the dilute-gas approximation really becomes good only for larger β than used in our experiments. Nevertheless, it is interesting to use this approximation to make rough estimates for the density of monopoles or monopole-antimonopole pairs at large β.

First, let us imagine a system consisting of a single cube of unit size. After gauge fixing, it has five independent link variables. The ground state of the system is $\theta_p = 0$ for each of the six plaquettes, while a one-monopole configuration can be

generated by placing 2π units of (outgoing) flux over the six plaquettes, along with -2π units of Dirac string in one face. The minimum-action configuration is symmetric: each face carries $\pi/3$ units of flux (plus a string somewhere). Since all $\cos\theta_p$ are equal to $\frac{1}{2}$,

$$M_{ij}(\text{monopole}) = \tfrac{1}{2} M_{ij}(\text{vacuum}) \tag{C6}$$

and

$$\rho_M = \sqrt{32}\, e^{-3\beta} . \tag{C7}$$

One may perform similar analyses for larger systems. For example, a monopole centered in a $3\times3\times3$ cube has a mass $m\beta$ [$m\beta \equiv S(\text{vac}) - S(\text{monopole})] \simeq (3+0.96)\beta$. In bigger systems one rapidly builds up the usual Coulomb self-energy of an isolated charge. For comparison with our Monte Carlo simulation, however, these calculations are probably unreliable: If the monopole density is too dilute, monopoles move too slowly for practical Monte Carlo calculation, and if the density is higher, interactions become important at long distance. A value $m \sim 3$ to 4 which takes into account only the short-distance part of the monopole field is probably a reasonable estimation for a monopole density when that density is such that monopole separation is typically only a few lattice spacings.

The density of monopole-antimonopole pairs is somewhat harder to estimate. In a universe of two cubes we have

$$M \equiv S(\text{vac}) - S(\text{pair}) = \left[\sum_{p_1} (1-\cos\theta_{p_1}) + \sum_{p_2} (1-\cos\theta_{p_2}) - (1-\cos\theta_{p_{12}})\right]\beta , \tag{C8}$$

where $p_{1,2}$ are plaquettes on the two cubes which share plaquette p_{12}. While each cube separately has a minimum configuration at $\theta_p = \pi/3$, the system may lower M by increasing the flux through the shared face until the pair decays. For example, the symmetric combination ($\theta_p = \pi/3$) has $M = \frac{11}{2}\beta$, but a configuration with $\theta_{p_{12}} = \pi$, where all other $\theta_p = \pi/5$, has $M = 3.91$. This last figure represents a lower limit on the mass of an $M\bar{M}$ pair.

[1] K. G. Wilson, Phys. Rev. D 10, 2445 (1974); J. Kogut and L. Susskind, *ibid.* 11, 395 (1975).

[2] A. M. Polyakov, Nucl. Phys. B120, 429 (1977).

[3] T. Banks, R. Myerson, and J. Kogut, Nucl. Phys. B129, 493 (1977); R. Savit, Phys. Rev. Lett. 39, 55 (1977).

[4] K. Osterwalder and E. Seiler, Ann. Phys. (N.Y.) 110, 440 (1978); A. Guth, Phys. Rev. D 21, 2291 (1980).

[5] M. Creutz, L. Jacobs, and C. Rebbi, Phys. Rev. Lett. 42, 1390 (1979); Phys. Rev. D 20, 1915 (1979).

[6] M. Creutz, Phys. Rev. Lett. 43, 553 (1979); Phys. Rev. D 21, 1006 (1978); 21, 2308 (1978); K. G. Wilson, Cornell report, 1979 (unpublished); C. Rebbi, Phys. Rev. D 21, 3350 (1980); G. Bhanot and B. Freedman, Brookhaven report, 1980 (unpublished); G. A. Jongeward and J. D. Stack, Phys. Rev. D 21, 3360 (1980); S. Shenker and J. Tobochnik, Phys. Rev. B 22, 4462 (1980).

[7] S. Elitzur, R. B. Pearson, and J. Shigemitsu, Phys. Rev. D 19, 3698 (1979); D. Horn, M. Weinstein, and S. Yankielowicz, *ibid.* 19, 3715 (1979); A. Ukawa, P. Windey, and A. Guth, *ibid.* 21, 1013 (1980).

[8] N. Metropolis, A. Rosenbluth, M. Rosenbluth, A. Teller, and E. Teller, J. Chem. Phys. 21, 1087 (1953).

[9] Logarithmic corrections to the perimeter law were first noticed by E. Fradkin and L. Susskind, Phys. Rev. D 17, 2637 (1978). We thank John Cardy for a discussion on this point.

[10] A. Belavin, A. Polyakov, P. Schwartz, and Y. Tyupkin, Phys. Lett. 59B, 851 (1975); G. 't Hooft, Phys. Rev. D14, 3432 (1976); C. Callan, R. Dashen, and D. Gross, *ibid.* 20, 3279 (1979), plus references therein.

[11] J. José, L. P. Kadanoff, S. Kirkpatrick, and D. R. Nelson, Phys. Rev. B 16, 1217 (1977).

[12] J. Tobochnik and G. Chester, Phys. Rev. B 20, 3761 (1979).

[13] J. Cardy, Nucl. Phys. B (to be published).

[14] G.' t Hooft, Nucl. Phys. B153, 141 (1979).

[15] J. Groeneveld, J. Jurkiewicz, and C. P. Korthals Altes, Utrecht report, 1980 (unpublished).

[16] A. A. Migdal, Zh. Eksp. Teor. Fiz. 69, 810 (1975); 69, 1457 (1975) [Sov. Phys. JETP 42, 413 (1976); 42, 743 (1976)]; L. P. Kadanoff, Ann. Phys. (N.Y.) 100, 359 (1976).

[17] For a review of Monte Carlo methods applied to spin systems, see K. Binder, in *Phase Transitions and Critical Phenomena*, edited by C. Domb and M. S. Green (Academic, New York, 1976), Vol. 5B.